

Magnetization in short-period mesoscopic electron systems

Vidar Gudmundsson and Sigurdur I. Erlingsson

Science Institute, University of Iceland, Dunhaga 3, IS-107 Reykjavik, Iceland

Andrei Manolescu

Institutul Național de Fizica Materialelor, C.P. MG-7 București-Măgurele, România

We calculate the magnetization of the two-dimensional electron gas in a short-period lateral superlattice, with the Coulomb interaction included in Hartree and Hartree-Fock approximations. We compare the results for a finite, mesoscopic system modulated by a periodic potential, with the results for the infinite periodic system. In addition to the expected strong exchange effects, the size of the system, the type and the strength of the lateral modulation leave their fingerprints on the magnetization.

I. INTRODUCTION

Several different probes have been used to investigate the properties of the two-dimensional electron gas (2DEG) in the quantum Hall regime, transport and optical experiments, or equilibrium methods including capacitance and magnetization measurements, to name only a few. The magnetization of high mobility homogeneous 2DEG has been measured by two methods. One method uses sensitive mechanical, torque magnetometers.^{1,2} More recently, a low-noise superconducting quantum interference device (SQUID) has also been used.^{3,4,5} These precision measurements reveal many-body effects such as the exchange enhancement at odd filling factors⁶ and the fractional quantum Hall effect and, in addition, an unidentified effect around filling factor $\nu \approx 2$ that might be connected to skyrmions.⁵

These experimental techniques are expected to be used soon for measuring the magnetization in lateral superlattices. The magnetization has been calculated for a disordered homogeneous 2DEG within the Hartree-Fock approximation (HFA)⁷ and within a statistical model for inhomogeneities corresponding to a Hartree approximation (HA).⁸ The results show strong exchange effects, already observed in experiments,^{2,4,5} and manifestations of the screening properties of the 2DEG.

Concerning periodic systems, the magnetization and the persistent current have been calculated by Kotlyar et. al. for a finite array of quantum dots using a Mott-Hubbard model for the electron-electron interactions, both intra-dot and inter-dot.^{9,10} In an infinite lateral superlattice, defined by a potential periodic in two directions (electric modulation) the energy spectrum in the presence of a magnetic field can only be calculated when the ratio of the magnetic flux through a lattice cell to the unit flux quantum, ϕ/ϕ_0 , is a rational number. The unit cell can then be enlarged to have an integer number of flux quanta flowing through it.¹¹ In principle, the magnetization of a 2DEG in a lateral superlattice can be evaluated in the thermodynamic limit as the negative derivative of the free energy with respect to the magnetic field B ,^{7,8} since the energy spectrum is always a continuous function of the flux.^{10,11,12} The inclusion of the Coulomb

interaction to the model, within a self-consistent scheme such as the HA¹³ or the HFA,¹⁴ does severely limit the possibility to effectively change the value of B by a small amount in order to take a numerical derivative. Nevertheless, such a thermodynamic calculation can be done for a modulation that varies only along one spatial direction, i. e. for an array of quantum wires.

In this paper we shall evaluate the magnetization of a 2DEG in a periodic potential corresponding to a weak density modulation in both, or in only one spatial direction. In other words our system is either an array of dots or antidots, or of parallel quantum wires, in most cases with a strong overlap. We first consider a finite system with boundaries, and then the unbound system.

For the finite system we are able to calculate the total magnetization. For the infinite system with a 2D potential we shall rather use the definition applicable to a mesoscopic system with a phase coherence length L_ϕ much larger than the spatial period of the square unit cell L . It is clear to us that in this manner we are calculating the contribution to the magnetization due to the periodic modulation, neglecting the contribution stemming from the edge of a real system. In an experiment the total magnetization is indeed measured and we would have a hard time arguing that the edge contribution is statistically insignificant in the thermodynamic limit. Our way out of this dilemma is to compare several results that we can obtain.

First, we compare the results for the finite system of various sizes, by heuristically separating the contribution of the bulk and edge current distributions to the total magnetization. Second, we compare quantitatively and qualitatively the bulk contribution in the finite system to the magnetization produced by one unit cell in the infinite system. We point out that experimentally it may be possible to measure only the contribution to the magnetization caused by the periodic modulation by placing the entire SQUID-loop well within the sample. And third, we compare to the total thermodynamic magnetization of an infinite system which is periodic in only one spatial direction and thus not subject to commensurability difficulties.

Our calculations show that the bulk contributions to

the magnetization are strongly dependent on the presence or absence of the exchange interaction in the models supporting the view of Meinel et. al. that magnetization is an ideal probe of the many-body effects in a 2DEG.⁵ Magnetization has been calculated for quantum Hall systems in the fractional regime with higher order approximations that reproduce more reliably exchange and correlation effects.^{15,16} Here we focus our attention on relatively large structured systems with several Landau bands included and have thus to resort to the HFA in order to make the calculation tractable in CPU-time. Recent comparison between results from exact numerical diagonalization and the HFA show that in high Landau levels the two approaches agree on the formation of charge density waves.¹⁷

We shall consider periodic potentials of a short period, 50 nm, which means short with respect to the present technical possibilities, but still realistic. In this case, for GaAs parameters and for magnetic fields in the range of few Tesla, the screening effects due to the direct Coulomb interaction are weak. However, the exchange effects remain strong, and they amplify the single-particle energy dispersion.¹⁴ Therefore the presence of the periodic potential should become prominent in the magnetization even for weak amplitudes. And last, but not least, by avoiding strong screening we are benefitted by a shorter computational time.

II. MODELS

The magnetization is calculated within three models in the paper, self-consistently with respect to the electron-electron Coulomb interaction: A finite model using the HA, an infinite model periodic in both spatial directions, using the unrestricted Hartree Fock approximation (UHFA), and an infinite model periodic in only one spatial direction, using the standard HFA.

A. Finite 2DEG

The model for a finite system consists of a laterally confined 2DEG. A hard wall potential ensures that the electrons stay in the square region

$$\Sigma = \{(x, y) | 0 < x < L_x, 0 < y < L_y\}, \quad (1)$$

the wave functions being zero at the boundary. An external modulating potential and a perpendicular magnetic field are applied. The potential has the form

$$V_{\text{sq}}(\mathbf{r}) = V_0 \left\{ \sin\left(\frac{n_x \pi x}{L_x}\right) \sin\left(\frac{n_y \pi y}{L_y}\right) \right\}^2, \quad (2)$$

where n_x and n_y count the number of dots in x and y direction respectively, giving in total $N_c = n_x n_y$ unit cells. The Schrödinger equation is solved by expanding

the eigenfunctions in Fourier sine-series and the expansion coefficients are found by diagonalizing the Hamiltonian matrix. The electron interaction is taken into account in the Hartree approximation.

The total magnetization can be calculated according to the definition for the orbital and the spin component of the magnetization,¹⁸

$$M_o + M_s = \frac{1}{2c\mathcal{A}} \int_{\mathcal{A}} d^2r (\mathbf{r} \times \langle \mathbf{J}(\mathbf{r}) \rangle) \cdot \hat{\mathbf{n}} - \frac{g\mu_B}{\mathcal{A}} \int_{\mathcal{A}} d^2r \langle \sigma_z(\mathbf{r}) \rangle, \quad (3)$$

where \mathcal{A} is the total area of the system. The equilibrium local current is evaluated as the quantum thermal average of the current operator,

$$\hat{\mathbf{J}} = -\frac{e}{2} \left(\hat{\mathbf{v}}|\mathbf{r}\rangle\langle\mathbf{r}| + |\mathbf{r}\rangle\langle\mathbf{r}|\hat{\mathbf{v}} \right), \quad (4)$$

with velocity operator $\hat{\mathbf{v}} = [\hat{\mathbf{p}} + (e/c)\mathbf{A}(\mathbf{r})]/m^*$, \mathbf{A} being the vector potential. Even though the magnetic field B can be varied freely in this model we have used the definition of the orbital magnetization (3) rather than evaluating the derivative of the free energy with respect to the magnetic field.

B. Periodic 2DEG in two directions

The two-dimensional modulation of the system is a square lattice of quantum dots ($V_0 > 0$) or antidots ($V_0 < 0$) determined by the static external potential

$$V_{\text{QAD}}(\mathbf{r}) = V_0 \left\{ \sin\left(\frac{gx}{2}\right) \sin\left(\frac{gy}{2}\right) \right\}^2, \quad (5)$$

or a simple cosine-modulation defined by

$$V_{\text{per}}(\mathbf{r}) = V_0 \{ \cos(gx) + \cos(gy) \}, \quad (6)$$

where g is the length of the fundamental inverse lattice vectors, $\mathbf{g}_1 = 2\pi\hat{\mathbf{x}}/L$, and $\mathbf{g}_2 = 2\pi\hat{\mathbf{y}}/L$. The Bravais lattice defined by V_{QAD} or V_{per} has a periodic length L and the inverse lattice is spanned by $\mathbf{G} = G_1\mathbf{g}_1 + G_2\mathbf{g}_2$, with $G_1, G_2 \in \mathbf{Z}$. The commensurability condition between the magnetic length ℓ and the period L requires magnetic-field values of the form $B = pq\phi_0/L^2$, with $p, q \in \mathbf{N}$, and $\phi_0 = hc/e$ the magnetic flux quantum.^{13,19} Arbitrary rational values can, in principle, be obtained by resizing the unit cell in the Bravais lattice.

For this model we evaluate the contribution of the periodic modulation to M_o and M_s , rather than the total magnetization. Using in Eq. (3) the periodicity of the current and spin densities, and the reflection symmetry of the unit cell, we reduce the integrations to a single cell. Obviously, in the absence of the modulation $\langle \mathbf{J}(\mathbf{r}) \rangle \equiv 0$ and the orbital contribution vanishes.

The ground-state properties of the interacting 2DEG in a perpendicular homogeneous magnetic field $\mathbf{B} = B\hat{\mathbf{z}}$

and the periodic potential are calculated within the UHFA for the Coulomb interacting electrons at a finite temperature.^{20,21} The approximation is unrestricted in the sense that the single-electron states do not have to be eigenstates of $\hat{\sigma}_z$.

C. Periodic 2DEG in one direction

The modulation is defined by the potential

$$V_{\text{per}}(x) = V_0 \cos\left(\frac{2\pi x}{L}\right), \quad (7)$$

describing an array of parallel quantum wires. In this case there is no restriction on the magnetic-field values, the magnetic flux through one lattice cell always being infinite. The groundstate is calculated in the HFA, by diagonalizing the Hamiltonian in the Landau basis, and by expanding the matrix elements in Fourier series. Therefore we can evaluate directly the total magnetization $M = M_o + M_s$ by the thermodynamic formula appropriate for the canonical ensemble,

$$M = -\frac{1}{\mathcal{A}} \frac{d}{dB}(E - TS), \quad (8)$$

where E is the total energy, and S the entropy. We shall assume the temperature is sufficiently low to neglect the second term of Eq. (8). In view of more realistic results we also assume a small disorder broadening of the Landau levels, which we take into account with a Gaussian model for the spectral function.⁷

III. RESULTS

The numerical calculations are performed with GaAs parameters, $m^* = 0.067$, and $\kappa = 12.4$. In the case of the infinite periodic modulation, in the UHFA, HFA, or the HA, the bare g -factor is -0.44 , and is set equal to zero in the model of the finite 2DEG in the HA. Mostly for numerical reasons we keep a finite temperature, which for the models with 2D potential is 1 K, and for the 1D potential is 0.2 K. In all cases the length of the unit cell is $L = 50$ nm.

A. Finite system with 2D potential

The magnetization for the finite system is shown in Fig. 1. The system size is progressively increased, starting from a single cell of 50×50 nm², to a system of 5×5 cells, keeping the unit-cell size constant. Each cell is defined by one period of the modulation potential (2). When the system consists of more than one cell we, ad hoc, divide the magnetization into an edge part M_e with a contribution only from the first row of cells around the system, and a bulk part M_b with the contribution from

the rest of the cells. Below we shall see that generally, the magnetization M_b does approach the orbital magnetization expected for a large system as the number of cells N_c is increased. The variable on the x -axis of the figure, N/N_c , i. e. the number of electrons in a single cell, can approximately be interpreted as a filling factor for the 3×3 and the 5×5 system. This is confirmed by the evolution of the chemical potential μ through the single electron Hartree-states depicted in Fig. 2. For even-integer values of N/N_c μ jumps through 'gaps' of sparsely distributed edge states separating states concentrated into precursors of Landau bands. The bulk M_b and the edge M_e contributions to the magnetization as well as the total magnetization are of similar magnitudes. However the oscillations of M_b around zero are more symmetric than those of M_e . This is because the direction of the edge current is more commonly as expected from the classical clockwise motion of the electrons around the sample, thus giving a preferred sign to M_e . Modestly increasing the size, from 3×3 to 5×5 unit cells, clearly gives the finite system more of the character of an extended system. The bulk magnetization for the large system is small when ν is not close to even integers due to the strong screening of the modulation potential away from the edges of the system. This is confirmed by Fig. 3 showing M_o of the noninteracting 5×5 system. The structures around even integer values of ν are less steep than for the interacting system. In the presence of the interaction the energy gaps are reduced by screening, which is self-consistently determined by the density of states around μ . When μ lies within one 'band' (i. e. ν is not an even integer) the Coulomb repulsion forces the electron density to spread out more evenly shifting the "effective filling" N/N_c a small amount. A slight change in the magnetic flux in the finite system only shifts the relation between the number of electrons and the effective filling factor.⁸

The current distribution for a 5×5 system is shown in Fig. 4 which reveals a strong edge current, but also a bulk current structured self-consistently in a complex way by the modulation, the interaction, and the location of μ with respect to the energy levels. This interplay of complex bulk contributions with the effects of the edge currents opens the question what are the effects of a modulation in an extended electron system on the magnetization.

B. Infinite system with 2D potential

Next, we turn our attention to the infinite system, that is modulated in two directions, and calculate the contribution to the magnetization from one unit cell. In Fig. 5 the total energy is shown as a function of the filling factor ν for the extended periodic 2DEG in the UHFA and the HA for the case $pq = 2$. Two magnetic flux quanta flow through the unit cell and each Landau band is split into two subbands which in turn are doubly spin split. Filling factor two means thus that both spin states of one Lan-

dau band are occupied, and in total four subbands are below the Fermi level. The modulation with $V_0 = 1.0$ or 0.1 meV is small compared to $\hbar\omega_c = 5.71$ meV. The minima in the total energy for the UHFA reflect the strong exchange interaction for electrons, added to nearly filled Landau bands or subbands thereof. Fig. 6 compares the total magnetization, Eq. (3), and its components M_o and M_s calculated within the UHFA, with the total magnetization according to the HA. The main difference between the results of these two approximations is the sharp reduction in the magnetization caused by the exchange interaction around odd integer filling factors. In this region the enhanced spin splitting of the subbands is larger than the subband splitting caused by the modulation. The order of the subbands (with respect to spin and magnetic subband index) and their curvature thus leads to M_o being of same sign for $\nu = 2.5$ and $\nu = 3.5$. The behavior is thus different around the even and odd values of ν . Later we see that this is not in the case of $pq = 1$. Just like for the total energy the different modulation strengths result in minor changes in M_o , because the energy dispersion of the Landau bands is determined by the exchange energy rather than by the external or screened potentials.¹⁴

The light effective mass and the small g -factor of electrons in GaAs cause the spin contribution M_s to be an order of magnitude smaller than the orbital one. A comparison of M_s in these two approximations can be seen in Fig. 7. In the case of the UHFA the exchange interaction always leads to the maximum spin polarization. In the HA the spin splitting of the Landau bands is only the bare Zeeman gap, here about 0.07 meV, i. e. much smaller than the intra-band energy dispersion which is of the order of the modulation amplitude, $V_0 = 1$ meV. Therefore the chemical potential is never able to lie only in one spin subband. New electrons are being added to the system concurrently, to both spin states, resulting in a reduced polarization.

In the case of one flux quantum through a unit cell ($pq = 1$) each Landau band consists of only two subbands, with different spin quantum numbers. This simpler band structure is reflected in the magnetization (see Fig. 8). Here the spin-bands hosting μ for the filling range $2.5 \leq \nu < 3$ and $3 < \nu \leq 3.5$ have opposite curvature causing a maximum and a minimum in M_o , respectively. For the lower ν range the Fermi level (μ) is in the lower spin subband of the second Landau-band pair, see Fig. 9. Here the Fermi contours ("Fermi surface") encircle the energy maxima at the edges of the Brillouin-zone (hole orbits), while for the higher ν range they close around the minimum of the upper spin subband (electron orbits).

In the case of two flux quanta each Landau band is fourfold split as can be seen in Fig. 10. For $\nu = 2.0$ only the splitting due to the modulation is clearly visible but for ν not equal to an even integer the spin splitting gets more enhanced due to the strong exchange force. Furthermore, we see that the subbands repel each other around the Γ point (center of the Brillouin zone) resulting in a different occurrence as ν is swept from 2.8 to

3.3 . In contrast to the strong ν -dependent interaction effects on the energy spectra we show in Fig. 11 the "static" energy bands of the noninteracting system that are independent of ν and the location of μ .

Around $\nu = 1$ the order of the Landau subbands is unusual. The states below the Fermi level are those of the Landau subband $(n, \sigma) = (0, +)$, n being the orbital and σ the spin quantum numbers. But the Landau subbands above, i. e. $(0, -)$ and $(1, +)$, are overlapped due to the strong exchange enhancement of the gaps between all the subbands with the same n but opposite σ . Therefore the first states which are populated for $\nu > 1$ belong to the subband $(1, +)$, while the subband $(0, -)$ is populated a bit later (for slightly higher ν). This situation is well known in the atomic physics of complex atoms, and has also been demonstrated in quantum dots, with a current-spin density-functional approach,²² which in principle is more reliable than our UHFA. In our case we observe this spin-state inversion as a small anomaly in M_s around $\nu = 1$, Fig. 8, where the maximum of M_s is shifted to $\nu > 1$.

The fact that the magnetization calculated by Eq. (3) for a unit cell in an infinite doubly modulated system reflects *only* the contribution of the modulation is seen in Fig. 12, where M for a dot and an antidot modulation of the same strength are mirror symmetric around zero for low ν . For higher ν the mixing of the Landau bands due to the Coulomb interaction slightly skews the mirror symmetry. For a homogeneous system ($V_0 = 0$) the persistent current in the definition of the magnetization (3) vanishes and thus M_o . Similar effect was seen for the bulk magnetization of the finite system in Fig. 1 for noninteger values of ν . Due to the enhancement of subband width caused by the exchange force the transition to zero magnetization with decreasing modulation does not happen in a smooth linear fashion.¹⁴

C. Correspondences between the finite and the infinite systems

Now we come back to the question how the magnetization of the finite and infinite system are related. The magnetization for the finite system can be calculated by either equation (3) or (8) giving the same results for the low temperature assumed here. The orbital magnetization M_o is compared for the finite system of different sizes to the result for a single unit cell in an extended system with the same type of modulation in Fig. 13, but with the interaction accounted for in different ways. If we first look at the results for the infinite periodic system we notice that the largest variation of M_o occurs for the UHFA and the smallest for the HA with the noninteracting case inbetween. This is in accordance with the screening properties mentioned earlier, in the HA the modulation is screened more effectively than in the UHFA. This result is in agreement with the simplistically defined bulk magnetization M_b of the finite system seen in Fig. 1, the main

difference being the sharp variation of M_b at even integer values of ν . Their presence indicates that even though the current density is only integrated over the "bulk" of the system the underlying energy spectrum is affected by the chemical potential μ traversing its edge states. To be able to get the unit cell of the two different systems to give the same magnetization the finite system has to be even larger, exhausting our means of computation.

The magnetization of both systems (and also of the 1D modulated system, see the next subsection) compares well with results derived from an older model of statistical inhomogeneities in a 2DEG that was used to explain effects caused by oscillating Landau level width due to the electrostatic screening.⁸

The main differences between the magnetization of our finite and infinite periodic systems are: *i*) the asymmetry around the zero line in the case of the finite system, and *ii*) the missing steepness of M_o around even integer filling factors ν for the infinite system. Earlier we saw that the asymmetry is influenced by the contribution from the "edge" of the finite system. The second difference can also be traced to the edge states. In the extended model there are no edge states between the Landau subbands. Their shape and curvature can thus change sharply with the motion of the chemical potential μ through them, the self-consistent screening and exchange effects minimize any gaps that might evolve around μ , which in turn prevents any sharp jumps in M_o . With this in mind it is clear that *the magnetization for a realistic (large, but finite) modulated system is not simply the sum of the magnetization produced by two independent subsystems, the edge and the bulk.* The Coulomb interaction makes the separation of the contributions to M a nontrivial problem, which can be solved only by an experiment. In addition, we have seen that the self-consistent motion of μ through the energy bands depends strongly on the approximation used for the electron interaction.

D. Infinite system with 1D potential

We have noticed in our calculations that for the system sizes considered here the magnetization of the finite system is not strongly dependent on whether the modulation is assumed 2D as here, or 1D.²³ For an infinite system with a 1D modulation we can calculate the thermodynamically defined magnetization (8) presented in Fig. 14. As mentioned before we see here that M_o for the finite system, especially when it is enlarged, bears a strong similarity with M_o for the infinite 1D modulated 2DEG.

The calculation of the ground state for a modulated 2DEG with arbitrary magnetic fields is impossible for the 2D potential, due to the commensurability restrictions. The problem can be circumvented for a 1D modulated system that we shall now turn our attention to, and formulate predictions of experimental results that can be used to test the importance of the exchange interaction.

For such a system we have access to the total magnetization, i. e. bulk plus edge, in the thermodynamic limit. In Fig. 14 we display results for the infinite system with a 1D potential, obtained with Eq. (8).

First we show the sawtooth profile in the absence of a modulation potential, reflecting the instability of the Fermi level in the energy gaps. The exchange interaction determines the spin splitting for odd filling factors, but also amplifies the jumps for even filling factors by almost a factor of two. The reason is the enhancement effect on both the spin gaps and the Landau gaps. For the same reason, in the presence of a modulation the jumps are only slightly reduced. Similarly, as for the 2D modulation, the exchange interaction also increases the energy dispersion of the Landau bands for noninteger filling factors, by lowering the energy of the occupied states, see Figs. 9 and 10. Hence, the band width depends on the position of the Fermi level inside an energy band. This fact prevents the coincidence of the Fermi level with a band edge (top or bottom), resulting in sharp cusps for ν close to integers. The sharpness is an effect of the exchange interaction in the vicinity of a van Hove singularity.

Some amount of disorder may indeed broaden such cusps. In addition, the magnetization jumps may now slightly increase, because of the smearing of the band edges by disorder, which helps the Fermi level to enter or to leave a Landau band. When the Fermi level lies in the middle of a band screening effects are important. In principle screening is important when the modulation period is much bigger than the magnetic length and/or when high Landau bands, with extended wave functions, are occupied. However, even here we can see some oscillations in the upper bands, with orbital quantum number $n = 2$.

Increasing the modulation amplitude, from $V_0 = 1.5$ meV to $V_0 = 5$ meV we first see that the magnetization for the bands with $n = 1$ is relatively stable. Just like in Figs. 5 and 6, this is because the exchange amplification of the energy dispersion depends on the filling factor, rather than on the modulation amplitude.¹⁴ The spin splitting survives now only for $\nu = 3$, and it is abruptly suppressed for $\nu \geq 5$. A similar suppression occurs for $V_0 = 1.5$ meV, but at a higher ν , and it can be explained by the inflation of the wave functions in high Landau levels which rapidly equilibrates the number of spin-up and spin-down electrons and destroys the enhancement of the spin gap.²⁴ Such a suppression effect has been recently observed in magnetotransport experiments on short-period modulated systems, in the Shubnikov - de Haas peaks.²⁵

IV. FINAL REMARKS

We have calculated the magnetization of periodic systems and discussed with examples various properties of it due to system boundaries, periodicity, and Coulomb interaction. We have compared the results of the finite and

infinite systems and of the periodic systems in one and two spatial directions. Our aim is to provide information for understanding the magnetization measurements in mesoscopic systems, which are expected to become a new direction of experimental investigations.

Unlike in other types of experiments, like transport or electromagnetic absorption, the magnetization measurements seem to open a better and more direct access to the intrinsic, quantum electronic structure of the system. In transport experiments this is often intermediated by complicated electron-impurity interactions, and in far-infrared absorption usually the classical collective motion of the electron system is dominant. We have identified in the magnetization several properties of the energy spectrum which are absent or incompletely observed in transport or absorption measurements, like the exchange enhancement of the energy dispersion or the curvature of the Landau bands. According to a recent prediction the exchange effects may also determine hysteresis properties when acting on the energy dispersion, either by vary-

ing the modulation amplitude, or by varying the Zeeman splitting in tilted magnetic fields, and keeping the filling factor constant.¹⁴ The magnetization measurements could be the best suited tool for probing such effects. The present calculation further indicates that sought after delicate internal structure of the Landau bands, such as the Hofstadter butterfly,^{11,13,26} in a doubly periodic 2DEG might be better observed by magnetization than transport experiments.²⁷

Acknowledgments

This research was supported by the Icelandic Natural Science Foundation and the University of Iceland Research Fund. In particular we acknowledge additional support from the Student Research Fund (S. E.), NATO Science Fellowship (A. M.), and Graduiertenkolleg "Physik Nanostrukturierter Festkörper" (V. G.).

-
- ¹ J. P. Eisenstein *et al.*, Physical Review Letters **55**, 875 (1985).
- ² S. A. J. Wieggers *et al.*, Physical Review Letters **79**, 3238 (1997).
- ³ D. Grundler, I. Meinel, F. S. Bargsteadt, and D. Heitmann, Physica B **249-251**, 693 (1998).
- ⁴ I. Meinel *et al.*, 24th ICPS Israel ?? (1998).
- ⁵ I. Meinel, T. Hengstmann, D. Grundler, and D. Heitmann, Physical Review Letters **82**, 819 (1999).
- ⁶ T. Ando and Y. Uemura, J. Phys. Soc. Japan **37**, 1044 (1974).
- ⁷ A. H. MacDonald, H. C. A. Oji, and K. L. Liu, Phys. Rev. B **34**, 2681 (1986).
- ⁸ V. Gudmundsson and R. Gerhardts, Phys. Rev. B **35**, 8005 (1987).
- ⁹ R. Kotlyar and S. D. Sarma, Phys. Rev. B **55**, R10205 (1997).
- ¹⁰ R. Kotlyar, C. A. Stafford, and S. D. Sarma, Phys. Rev. B **58**, 3989 (1998).
- ¹¹ R. D. Hofstadter, Phys. Rev. B **14**, 2239 (1976).
- ¹² R. Ketzmerick, K. Kruse, F. Steinbach, and T. Geisel, Phys. Rev. B **58**, 9881 (1998).
- ¹³ V. Gudmundsson and R. R. Gerhardts, Phys. Rev. B **52**, 16744 (1995).
- ¹⁴ A. Manolescu and V. Gudmundsson, Phys. Rev. B **59**, 5426 (1999).
- ¹⁵ R. Haussmann, Phys. Rev. B **56**, 9684 (1997).
- ¹⁶ A. MacDonald and J. J. Palacios, Phys. Rev. B **58**, R10171 (1998).
- ¹⁷ E. H. Rezayi, F. D. M. Haldane, and K. Yang, Evidence of charge density wave ordering in half filled Landau levels, cond-mat/9903258, 1999.
- ¹⁸ J. Desbois, S. Ouvry, and C. Texier, Persistent Currents and Magnetization, cond-mat/9801106, 1998.
- ¹⁹ H. Silberbauer, J. Phys. C **4**, 7355 (1992).
- ²⁰ E. K. U. Gross, E. Runge, and O. Heinonen, *Many-Particle Theory* (Adam Hilger, Bristol, 1991).
- ²¹ J. J. Palacios *et al.*, Phys. Rev. B **50**, 5760 (1994).
- ²² O. Steffens, U. Roessler, and M. Suhrke, Europhys. Lett. **42**, 529 (1998).
- ²³ The finite system with 1D modulation has been discussed in: S. I. Erlingsson, A. Manolescu, and V. Gudmundsson, Proceedings of the 13th EP2DS, Ottawa (1999), Physica E in press.
- ²⁴ A. Manolescu and R. R. Gerhardts, Phys. Rev. B **51**, 1703 (1995).
- ²⁵ F. Petit *et al.*, Europhys. Lett. **38**, 225 (1997).
- ²⁶ V. Gudmundsson and R. R. Gerhardts, Phys. Rev. B **54**, 5223R (1996).
- ²⁷ T. Schlösser, K. Ensslin, J. P. Kotthaus, and M. Holland, Europhys. Lett. **33**, 683 (1996).

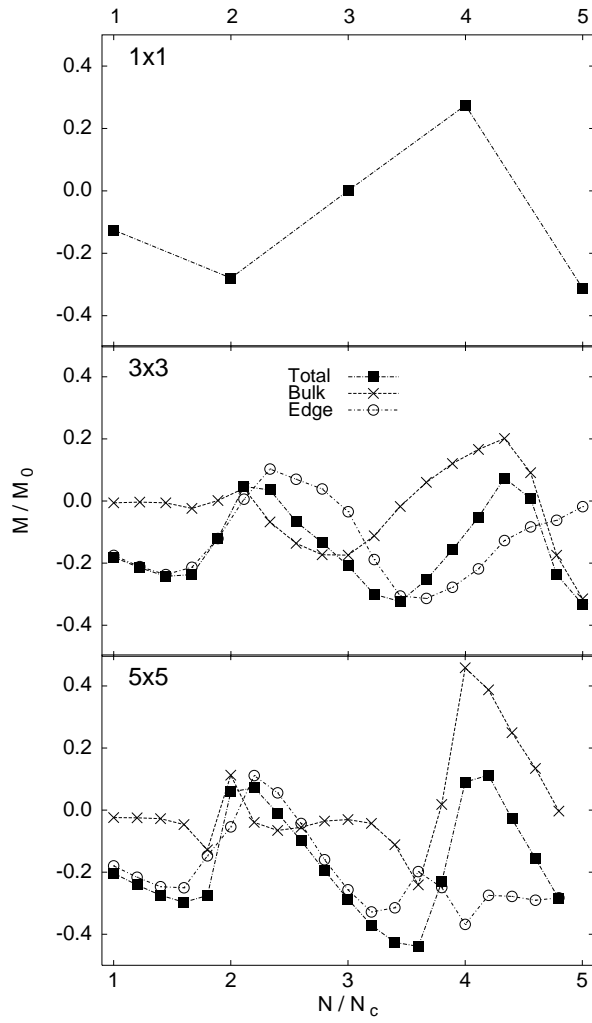


FIG. 1: The total (orbital) M_o , the bulk M_b , and the edge M_e magnetizations of a system of N electrons in $n_x \times n_y = N_c$ unit cells (HA). $pq=1$, $B \approx 1.65$ T, $M_0 = \mu_B^*/(L_x L_y)$, $V_0 = -1$ meV.

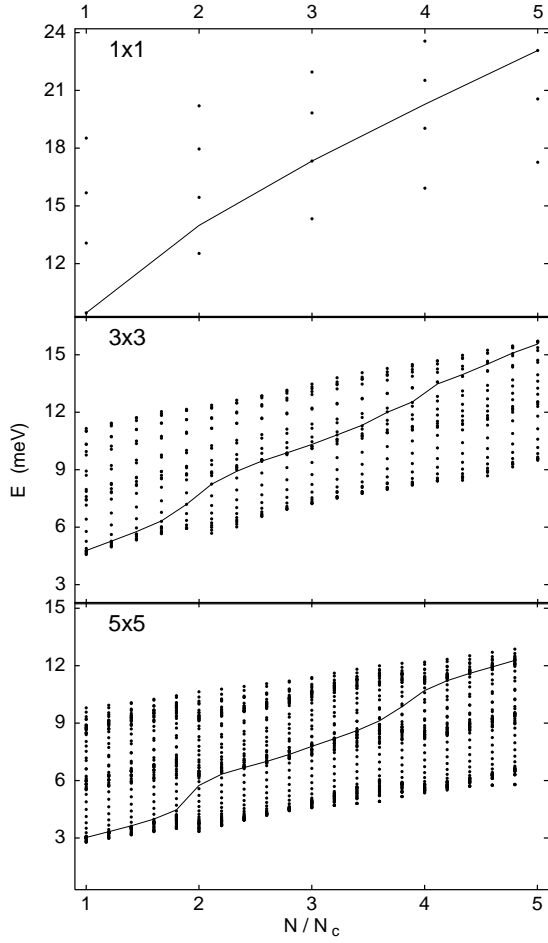


FIG. 2: The energy spectra (dots) for N electrons and the chemical potential μ (solid) for $n_x \times n_y = N_c$ arrays of quantum dots, (HA). $pq=1$, $B \approx 1.65$ T, $V_0 = \pm 5$ meV.

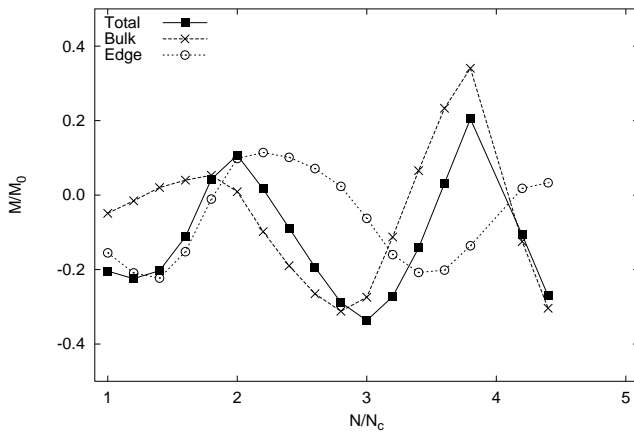


FIG. 3: The total (orbital) M_o , the bulk M_b , and the edge M_e magnetizations of a noninteracting system of N electrons in 5×5 unit cells (HA). $pq=1$, $B \approx 1.65$ T, $M_0 = \mu_B^*/(L_x L_y)$, $V_0 = -1$ meV.

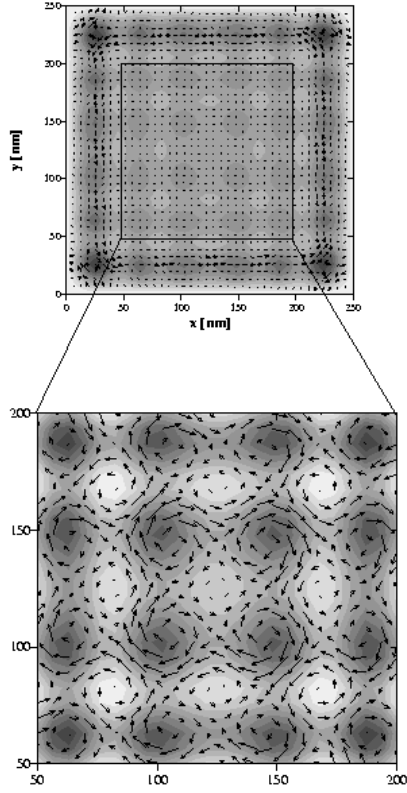


FIG. 4: The current (arrows) and electron density (contour) in a finite system of 5×5 unit cells (HA) for $N/N_c = 2.2$ (filling factor). $pq=1$, $B \approx 1.65$ T, $V_0 = -5$ meV.

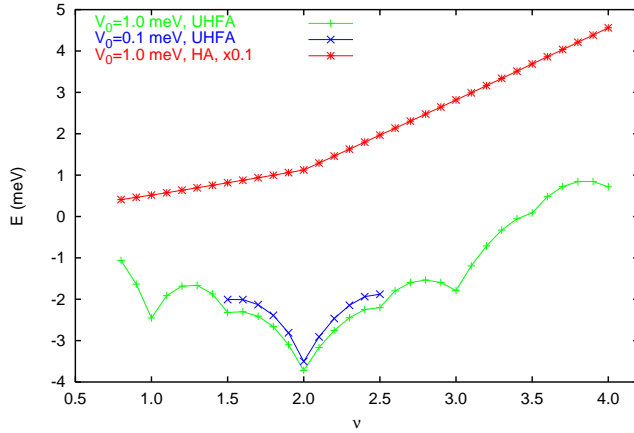


FIG. 5: The total energy per unit cell of the electron system in the case of the simple cosine-modulation (6) as a function of the filling factor ν for the UHFA and HA. (+) $V_0 = 1.0$ meV, and (x) $V_0 = 0.1$ meV. In case of the HA the total energy is multiplied by 0.1. $pq=2$, $B \approx 3.3$ T.

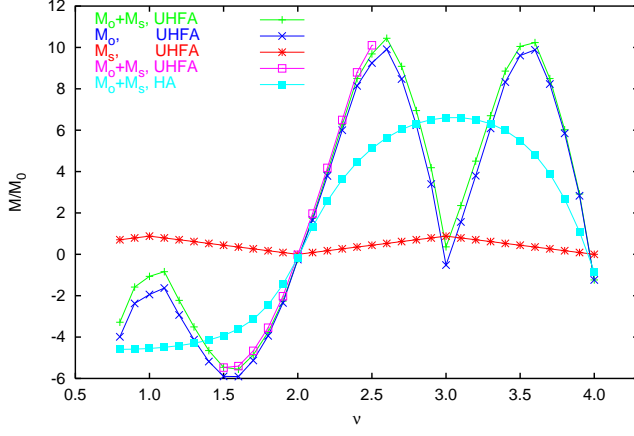


FIG. 6: The orbital M_o , and spin M_s contribution to the total magnetization for the simple cosine-modulation (UHFA) (6) with (+) $V_0 = 1.0$ meV, and (\square) $V_0 = 0.1$ meV, and the total magnetization in the HA for $V_0 = 1.0$ meV, as a function of the filling factor ν . $pq=2$, $B \approx 3.3$ T, $M_0 = \mu_B^*/(L_x L_y)$.

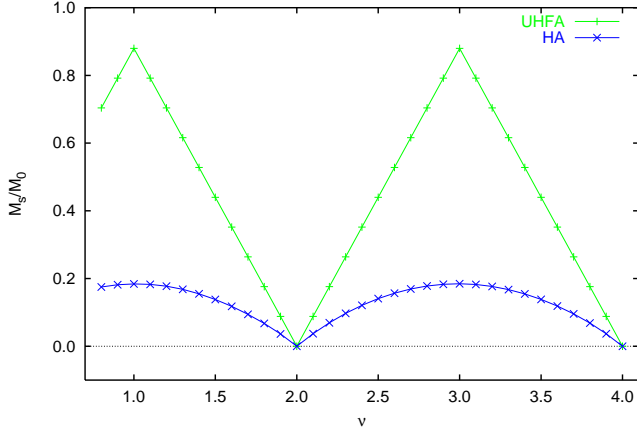


FIG. 7: The spin contribution to the magnetization M_s of the electron system in the case of the simple cosine-modulation (6) for the UHFA and the HA as a function of the filling factor ν . $pq=2$, $B \approx 3.3$ T, $V_0 = 1.0$ meV.

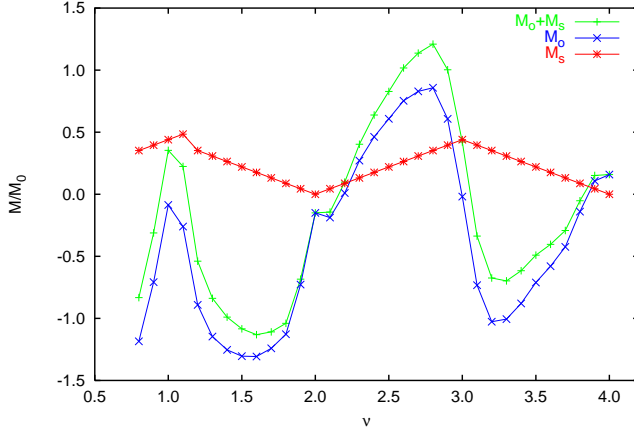


FIG. 8: The orbital M_o , and spin M_s contribution to the magnetization for the simple cosine-modulation (6) as a function of the filling factor ν . UHFA, $pq=1$, $B \approx 1.65$ T, $V_0 = 0.1$ meV.

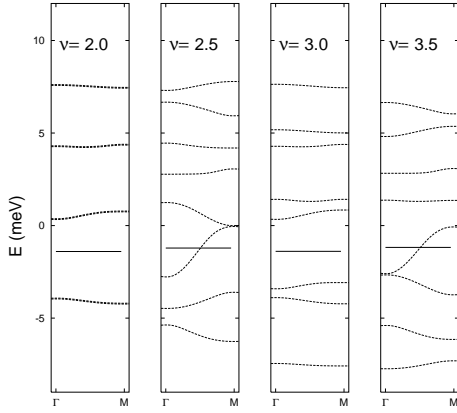


FIG. 9: Sections (Γ - M) of the energy spectra for the dot modulated interacting 2DEG. The chemical potential is indicated by a horizontal solid line. UHFA, $pq=1$, $B \approx 1.65$ T, $V_0 = -1.0$ meV.

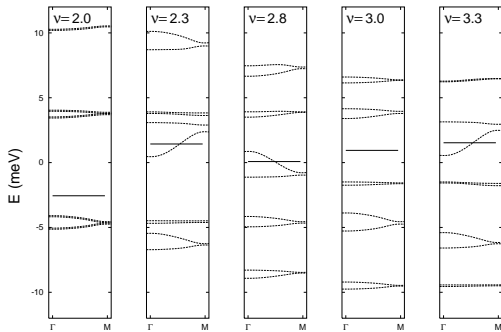


FIG. 10: Sections (Γ - M) of the energy spectra for the simple cosine modulated interacting 2DEG. The chemical potential is indicated by a horizontal solid line. UHFA, $pq=2$, $B \approx 3.3$ T, $V_0 = 1.0$ meV.

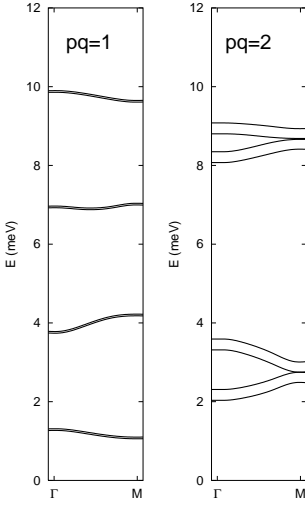


FIG. 11: Sections of the noninteracting energy spectra corresponding to the two interacting cases in Figures 9 and 10. The small spin splitting is not visible for the lower magnetic flux, $pq = 1$.

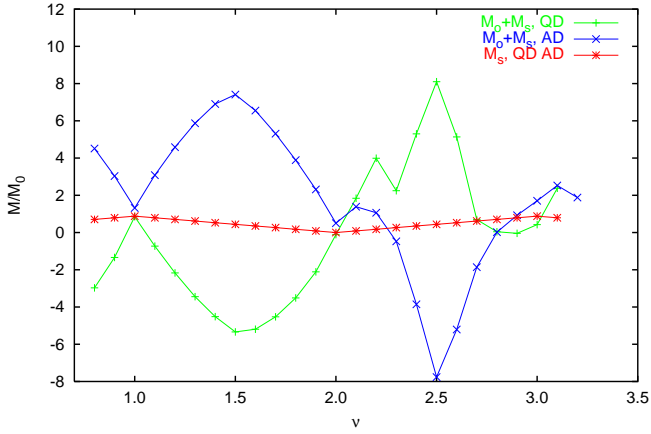


FIG. 12: The orbital M_o , and spin M_s contribution to the magnetization for a quantum dot (QD), and an antidot (AD) array (5) as a function of the filling factor ν . UHFA, $pq=2$, $B \approx 3.3$ T, $V_0 = \pm 5$ meV.

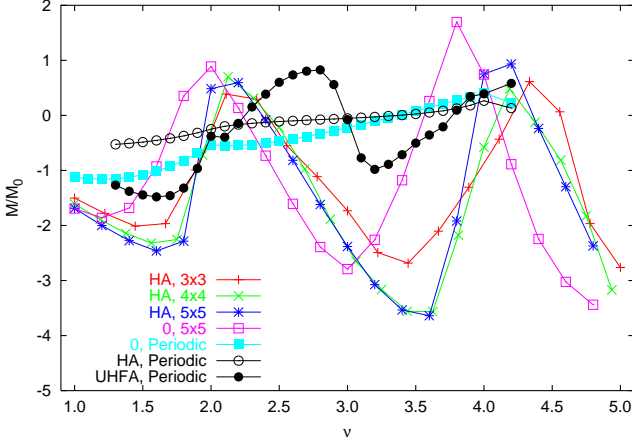


FIG. 13: The orbital magnetization M_o for the dot array (5) in UHFA, HA, and for noninteracting electrons compared to M_o for a finite systems of $n \times n$ unit cells in HA as a function of the filling factor ν . (For the finite system ν is approximated). $pq=1$, $B \approx 1.65$ T, $V_0 = -1$ meV.

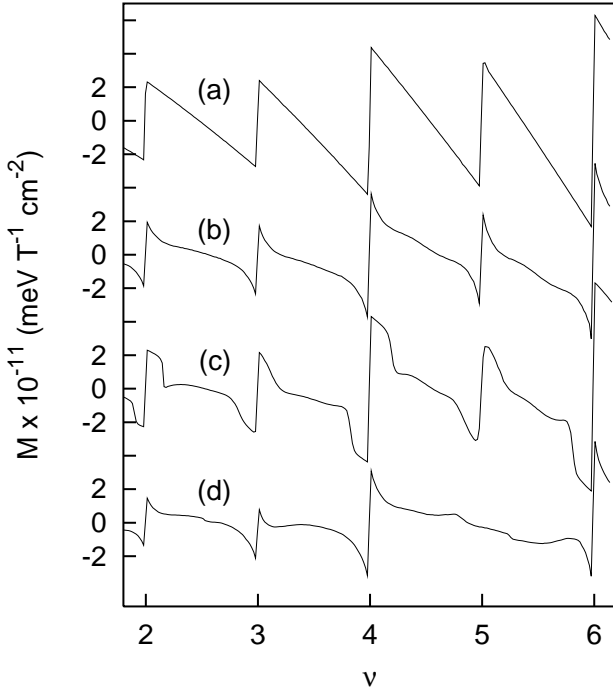


FIG. 14: (a) The sawtooth magnetization for the homogeneous 2DEG in the HFA, with exchange-enhanced spin splitting. $B = 3$ T. (b) The effect of a one-dimensional modulation with $V_0 = 1.5$ meV. (c) The effect of a disorder broadening $\Gamma = 2.6$ meV for the same modulation amplitude. (d) A modulation with $V = 5$ meV, suppressing the exchange enhancement of the spin splitting for $\nu = 5$ ($\Gamma = 0$).